

A Novel Radar Waveform Design for Suppressing Autocorrelation Side-Lobe Based on Chaotic and Single Fusion Encoding Method

Ji Li¹, Min Liu¹, Jianping Ou², and Wei Wang^{1, *}

Abstract—Multi-carrier Phase Coded (MCPC) signal has the advantages of large time-bandwidth product, low intercept, anti-jamming, digitization, flexible waveform, and high spectral utilization, and has become a hotspot in radar waveform research. However, MCPC signal has high-distance sidelobes which are difficult to suppress, after pulse compression processing. Excessive sidelobes will mask the existence of small and weak targets, thus losing the target signal, which limits the practical application of MCPC signals. Therefore, it is of great significance and practical value to study the sidelobe suppression of MCPC signals. From the point of view of waveform design, a multi-carrier phase-encoded signal combining chaotic encoding and single encoding (MCPC-CS) is designed by using chaotic sequence as phase encoding of MCPC signal and optimizing it. In this paper, peak sidelobe level ratio (PSLR) is used as a evaluation factor of the autocorrelation function. The simulation results show that MCPC-CS signal has a good autocorrelation peak sidelobe level ratio, and the autocorrelation sidelobe is reduced by more than 3 dB compared with the normal MCPC signal.

1. INTRODUCTION

The range resolution and detection ability of radar are the most important characteristics of radar signals. Increasing the pulse width increases the range of the radar signal, but this technique reduces the resolution. Therefore, in order to improve resolution, pulse width [1] must be reduced. To balance the distance and resolution, a usual solution is to compress the transmitted waveform [2]. However, after pulse compression processing of radar waveforms, distance sidelobes will be generated [3]. Excessive sidelobe will seriously affect the detection of weak target signal, resulting in signal loss [4]. In complex electromagnetic environment, the existing autocorrelation sidelobe level is still high after compressing the emitted waveform pulse, which is difficult to meet the practical application. Therefore, it is very important to design a signal with low sidelobe distance after pulse compression [5].

Multicarrier signals have lower bandwidth than single-carrier signals. Therefore, using multicarrier or multicarrier technology as radar transmission waveform can reduce bandwidth requirements, such as Orthogonal Frequency Division Multiplexing (OFDM) technology [6]. The principle of OFDM technology is to modulate a single carrier transmission signal to multiple carriers [7] and transmit it after superposition. The signal processed by OFDM technology has orthogonal overlap between subcarriers, so it has high frequency band utilization. Multicarrier phase coded (MCPC) signal combines OFDM technology with phase coding technology, so it will have a large time bandwidth product. Large bandwidth can improve the range resolution, and large time width can provide the required energy for the radar when it detects long-range targets. MCPC waveform design is complex and flexible. It has multidimensional modulation to improve pulse pressure gain and distance resolution. In addition, MCPC has advantages such as strong clutter suppression and anti-interference performance [8–10].

Received 22 April 2022, Accepted 1 June 2022, Scheduled 19 June 2022

* Corresponding author: Wei Wang (wangwei@csust.edu.cn).

¹ College of Computer and Communication Engineering, Changsha University of Science & Technology, Changsha 410000, China.

² College of Electronic Science and Technology, National University of Defense Technology, Changsha 410000, China.

Therefore, it has received wide attention. However, MCPC signal has a fatal disadvantage. In pulse compression processing, it will produce too high autocorrelation sidelobe level, and this sidelobe is difficult to be reduced by traditional methods. This will submerge the weak echo target in the high sidelobe and affect the detection ability of the radar.

Some scholars have studied the autocorrelation sidelobe suppression of multi-carrier and multi-carrier frequency signals. Li et al. [11], and Yang and Tao [12] suppressed the sidelobe by adjusting the subcarrier constellation points. Khan and Yoo [13] used additive signal sidelobe reduction technology and genetic algorithm to reduce the sidelobe to 35 dB, but the calculation is too complex. Tom et al. [14] added a cyclic prefix to the OFDM symbol to suppress autocorrelation sidelobes. Although the above methods can well reduce the autocorrelation sidelobe of multi-carrier signals, they are limited to non-radar applications. Prasanth [15] combined Zadoff-Chu sequence [16] with signal cancellation [17], which can reduce the autocorrelation sidelobe level by 3.28 dB, but this method is limited to 5 subcarriers. Gopalkrishna et al. [2] fused Hill mode and geometric series method to reduce the autocorrelation sidelobe with a large number of subcarrier sequences by 4.22 dB.

In this paper, Logistic chaotic sequence is used as phase coding to modulate MCPC signal. Compared with the traditional phase coding sequence, chaotic sequence includes polyphase P3, P4 code and two-phase Barker code. It has the characteristics of easy generation and large quantity [18], random and deterministic form, difficult prediction [19], and can improve the confidentiality of the system. Therefore, it is generally used in the field of cryptography and secure communication [20]. Li et al. [21] used Logistic chaotic sequence to modulate MCPC radar signal, but they focused on how to improve the anti-jamming performance of MCPC signal.

From the perspective of waveform design, this paper studies the influence of Logistic chaotic sequence on MCPC autocorrelation sidelobe level. Moreover, this paper creatively fuses chaotic coding sequence with single coding sequence and designs a multi-carrier phase-encoded signal combining chaotic encoding and single encoding (MCPC-CS). The ambiguity function of MCPC-CS signal is deduced, and the autocorrelation performance of MCPC-CS signal is compared with that of normal MCPC signal. The simulation results show that the pulse compression sidelobe of the signal is improved, and because it is derived from MCPC signal, it also inherits other advantages of MCPC signal, such as better anti-jamming ability than LFM signal.

2. MCPC-CS SIGNAL MODEL AND AMBIGUITY FUNCTION

The MCPC signal is composed of N subcarrier signals with M phase-coded sequences on each subcarrier, where each chip width is equal, and the interval between two adjacent subcarrier frequencies is equal to the inverse of the width of a single chip to achieve orthogonality between subcarriers.

Taking a single pulse as an example, the complex envelope expression of MCPC signal is expressed as:

$$s_c(t) = \sum_{n=1}^N \sum_{m=1}^M \omega_n b_{n,m} \text{rect}[t - (m-1)t_b] \exp[j2\pi(n-1)\Delta f_b t] \quad (1)$$

where $\text{rect}(t) = \begin{cases} 1, & 0 \leq t \leq t_b \\ 0, & \text{other} \end{cases}$. N is the number of subcarriers. M is the number of symbols. ω_n is the complex weighting factor of the n th subcarrier. $b_{n,m} = e^{j\phi_{n,m}}$ is the chaotic phase encoding of the M symbol in the N subcarrier. $\phi_{n,m}$ is the phase in the M symbol of the N subcarrier. t_b is the time width of each symbol. The subcarrier frequency interval Δf equals the inverse of the code width t_b , that is, $\Delta f = 1/t_b$. This is done to ensure the orthogonality between the carriers of the MCPC signal.

Based on formula (1), the general expression for MCPC-CS signal is:

$$s(t) = \sum_{n=1}^N \omega_n a_n \text{rect}(t) \exp[j2\pi(n-1)\Delta f_a t] + \sum_{n=1}^N \sum_{m=1}^M \omega_n b_{n,m} \text{rect}[t - (m-1)t_b] \exp[j2\pi(n-1)\Delta f_b t] \quad (2)$$

where a_n is a single encoding for the n th subcarrier. Δf_a and Δf_b are subcarrier frequency spacing of single coding and chaotic coding, respectively. The remaining parameters are the same as MCPC signal parameters.

The time-frequency structure diagram of MCPC-CS signal is shown in Figure 1.

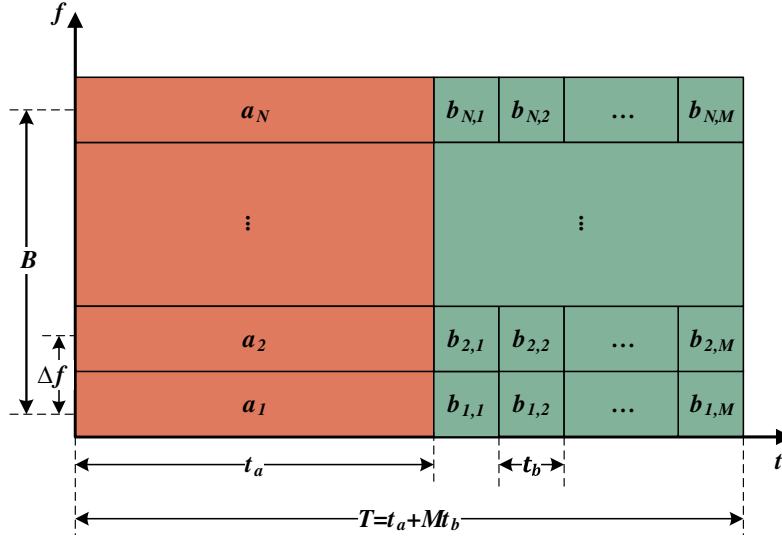


Figure 1. MCPC-CS time-frequency structure diagram.

Radar signal modulated by Logistic chaotic sequence has high resolution of range velocity, pin-like ambiguity function, and good anti-jamming ability [22]. a_n and $b_{n,m}$ in formula (2) are generated by an improved Logistic chaotic map whose mathematical expressions are:

$$x_{n+1} = 1 - 2x_n^2, \quad x_n \in [-1, 1] \quad (3)$$

The ambiguity, resolution, and suppression of clutter interference of radar waveforms are evaluated by an ambiguity function [23]. The ambiguity function is determined only by the radar transmission waveform and describes the output response of receiving the target echo by the target delay, Doppler frequency shift, and matched filter, that is:

$$\chi(\tau, \xi) = \int_{-\infty}^{+\infty} s(t)s^*(t + \tau) \exp(j2\pi\xi t) dt \quad (4)$$

Based on the definition of ambiguity function introduced in formula (4), combined with MCPC signal expression (1), MCPC signal ambiguity function can be derived:

$$\begin{aligned} \chi(\tau, f_d) &= \int_{-\infty}^{+\infty} s(t)s^*(t + \tau) \exp(j2\pi f_d t) dt \\ &= \int_{-\infty}^{+\infty} \sum_{n=1}^N \sum_{l=1}^N w_n u(t) \exp(j2\pi f_n t) w_l^* u(t + \tau)^* \exp[-j2\pi f_l(t + \tau)] \exp(j2\pi f_d t) dt \\ &= \sum_{n=1}^N \sum_{l=1}^N w_n w_l^* \exp(-j2\pi f_l \tau) \int_{-\infty}^{+\infty} u(t) u(t + \tau)^* \exp[j2\pi(f_n - f_l)t] \exp(j2\pi f_d t) dt \end{aligned} \quad (5)$$

When $n \neq l$ is a cross-ambiguity function, it can be ignored because the cross-ambiguity function is very small relative to the self-ambiguity function. When $n = l$ is a self-ambiguity function, the upper

form is the main body of the MCPC ambiguity function and can be written as:

$$\begin{aligned}\chi(\tau, f_d) &= \sum_{n=1}^N \omega_n^2 \exp(-j2\pi f_n \tau) \int_{-\infty}^{+\infty} u(t) u(t+\tau)^* \exp(j2\pi f_d t) dt \\ &= \sum_{n=1}^N \omega_n^2 \exp(-j2\pi f_n \tau) \sum_{q=-(M-1)}^{M-1} \chi_u(\tau - qt_b, f_d) \sum_{M-1}^{M-|q|} b_{n,m} b_{n,m+|q|}^* \exp(j2\pi f_d m t_b)\end{aligned}\quad (6)$$

where,

$$\chi_u(\tau, f_d) = \begin{cases} \exp[j\pi f_d(t_b - |\tau|)] \frac{\sin(\pi f_d(t_b - |\tau|))}{\pi f_d(t_b - |\tau|)} \left(1 - \frac{|\tau|}{t_b}\right), & |\tau| \leq t_b \\ 0, & |\tau| > t_b \end{cases}\quad (7)$$

Similarly, combined with the expression of MCPC-CS signal (2), the ambiguity function of single pulse signal is obtained:

$$\begin{aligned}\chi(\tau, f_d) &= \sum_{n=1}^N \omega_n^2 \exp(-j2\pi f_n \tau) \chi_u(\tau, f_d) a_n a_n^* \exp(j2\pi f_d t_a) \\ &\quad + \sum_{n=1}^N \omega_n^2 \exp(-j2\pi f_n \tau) \sum_{q=-(M-1)}^{M-1} \chi_u(\tau - qt_b, f_d) \sum_{M-1}^{M-|q|} b_{n,m} b_{n,m+|q|}^* \exp(j2\pi f_d m t_b)\end{aligned}\quad (8)$$

Figures 2(a), 2(b), and 2(c) are the ambiguity functions of linear frequency modulation signal, multicarrier chaotic phase-coded MCPC signal, and multicarrier phase-coded MCPC-CS signal combined with chaotic single coding. The blur function diagram of LFM signal with linear frequency modulation is “skewed edge”. There is distance Doppler coupling [24]. The ambiguity function of MCPC signal with multicarrier phase coding is “pushpin” with energy concentration effect. Since the MCPC-CS signal is an improvement on the MCPC signal, its ambiguity function graph has a “pushpin” like the MCPC signal. The ambiguity function graph of MCPC-CS signal is more concentrated near the origin than that of MCPC signal, and the autocorrelation sidelobes are evenly distributed, so it has better target resolution and higher measurement accuracy.

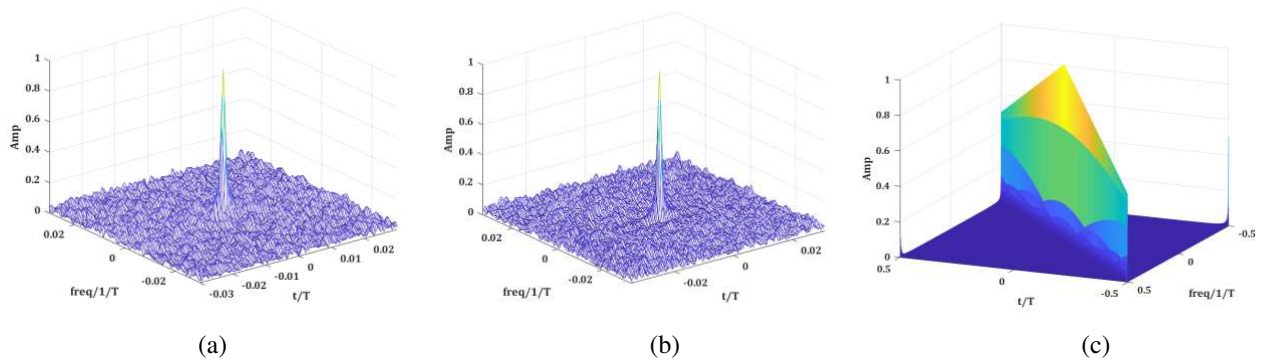


Figure 2. Three-dimensional ambiguity figure. (a) MCPC-CS, (b) MCPC, (c) LFM.

3. MCPC-CS SIGNAL DESIGN METHOD

The expression of the ambiguity function (4) shows that the ambiguity function is a two-dimensional function related to the time delay τ and the Doppler frequency shift ξ . When only the distance resolution of the signal needs to be studied, $\xi = 0$ can be chosen to obtain the ambiguity function $\chi(\tau, 0)$ in the distance dimension. The distance dimension ambiguity function is the signal autocorrelation function

$A(\tau)$, which can be used to represent the target distance resolution. When $\tau \neq 0$, as the autocorrelation sidelobe value decreases, the distance resolution to the target increases. Generally, the signal resolution is expressed as a normalized autocorrelation function (ACF). The expression for the autocorrelation function $A(\tau)$ is:

$$A(\tau) = \int_{-\infty}^{+\infty} s(t)s^*(t + \tau)dt \quad (9)$$

Its discrete form is:

$$A(k) = \sum s(p)s^*(p + k) \quad (10)$$

In Equation (8), when the Doppler frequency shift $f_d = 0$, the autocorrelation function of MCPC-CS signal can be obtained:

$$\begin{aligned} \chi(\tau, 0) = & \sum_{n=1}^N \omega_n^2 a_n a_n^* \exp(-j2\pi f_n \tau) \chi_u(\tau, 0) \\ & + \sum_{n=1}^N \omega_n^2 \exp(-j2\pi f_n \tau) \sum_{q=-(M-1)}^{M-1} \chi_u(\tau - qt_b, 0) \sum_{M-1}^{M-|q|} b_{n,m} b_{n,m+|q|}^* \end{aligned} \quad (11)$$

According to the above formula, the autocorrelation function of MCPC-CS signal is related to the number of chips M . Set $M = 1 : 40$, pulse compress the MCPC signal respectively, and the variation of autocorrelation sidelobe value with chip number is shown in Figure 3.

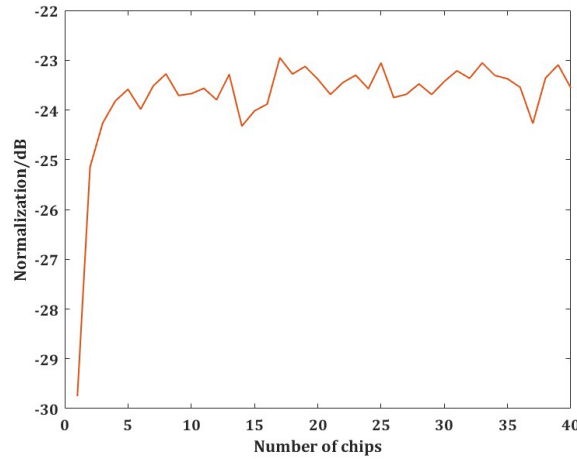


Figure 3. Effect of chip number on PSLR.

When M is 1, the minimum pulse pressure sidelobe of MCPC signal based on chaotic coding is about -29 dB. With the increase of the number of chips, the autocorrelation sidelobe increases and gradually stabilizes near -23 dB.

It can be seen from Figure 3 that the autocorrelation sidelobe of MCPC signal is the lowest only when $M = 1$. In this paper, MCPC signal at this time is called single coded MCPC signal. The single coded MCPC signal has only one symbol. Although the autocorrelation performance is the best, the chaotic code generated under the same broadband product is unchanged, which loses the original advantages of randomness and confidentiality of chaotic coding. Therefore, this paper uses the advantages of single coding and mixed modulation with chaotic sequences with chip number greater than 1 ($M = 40$), and designs a multi carrier phase coded MCPC-CS signal combining chaotic coding and chaotic single coding.

The MCPC-CS signal is designed by two-step screening method. Due to the randomness of chaotic sequences, the autocorrelation performance of different pulse signals is different. Therefore, the chaotic sequences with good autocorrelation need to be selected in the first round of screening.

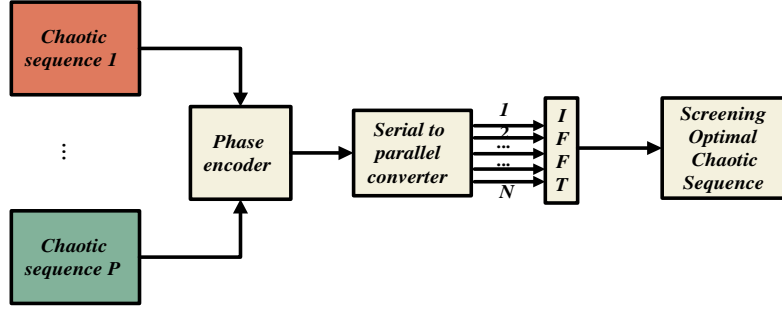


Figure 4. Screening chaotic sequences.

The first round of screening process is shown in Figure 4. The specific steps are as follows: firstly, P chaotic sequences are generated, and the sequences are modulated into phase coded signals through the phase encoder. Then, after serial to parallel converter and IFFT, the signals are transformed from frequency domain to time domain, the phase coded signals are autocorrelated, and the single coding and chaotic coding with the lowest peak sidelobe level are selected. The sampling length of the two coded signals is K and enter the second round of screening.

In the second round, the single coded signal and chaotic coded signal are combined into MCPC-CS signal to screen the MCPC-CS signal with the best autocorrelation sidelobe. The specific steps are as follows: make the sampling bits of the single coded signal k ($1 < k < K$) and change the proportion of the single coded signal in the MCPC-CS signal through the k value. After K iterations, the combined signal with the lowest PSLR value and the best anti-interference performance is selected.

The phase coded signal of the second round is distributed on each subcarrier, and then the signal is converted into analog signal through the parallel to serial converter and D/A conversion. Finally, the signal is moved to RF and transmitted through antenna. This is the generation process of MCPC-CS signal.

4. SIMULATION ANALYSIS

4.1. Performance Analysis of Anti-Replication Forwarding Interference

Replication Forwarding Interference (RFI) refers to copying the intercepted radar transmission signal, adding the parameter information of false target and sending it back to the radar receiver [25, 26]. In order to solve the severe challenge of all kinds of jamming faced by radar, it is necessary to require the signal transmitted by radar terminal to have strong anti-jamming ability.

Analyse the interference suppression of LFM signal and MCPC signal and set the simulation parameters: time width $t = 2 \mu\text{s}$, bandwidth $B = 500 \text{ MHz}$, chip number $M = 40$, SNR = -6 dB , and window function Hamming window. The Signal Jamming Ratio (SJR) improvement factor is introduced to evaluate the anti-interference ability of the signal. The expression is:

$$\delta_{SJR} = SJR_{PC} - SJR \quad (12)$$

where SJR_{PC} is the value of SJR after pulse compression.

In order to prove that the anti-copying and forwarding interference performance of waveform designed in this paper can adapt to different noise environments, we added Gaussian noise of different sizes to echo signal and interference signal, namely $-24 \text{ dB} \sim 6 \text{ dB}$, and set the step size to 3 dB . This section uses Monte Carlo simulation experiment to calculate the SJR improvement factor, and the simulation times are 1000 times. Monte Carlo simulation experiment is also called computer stochastic simulation method. It refers to the inherent randomness of the problem solved, which can be directly simulated with the computing power of the computer. The randomness of Gaussian noise will bring uncertainty to the experimental results. Therefore, this paper introduces this method to solve the uncertainty, so as to make the experimental results more rigorous.

The mean value of SJR improvement factor under 1000 Monte Carlo simulations of pulse pressure signal is shown in Figure 6.

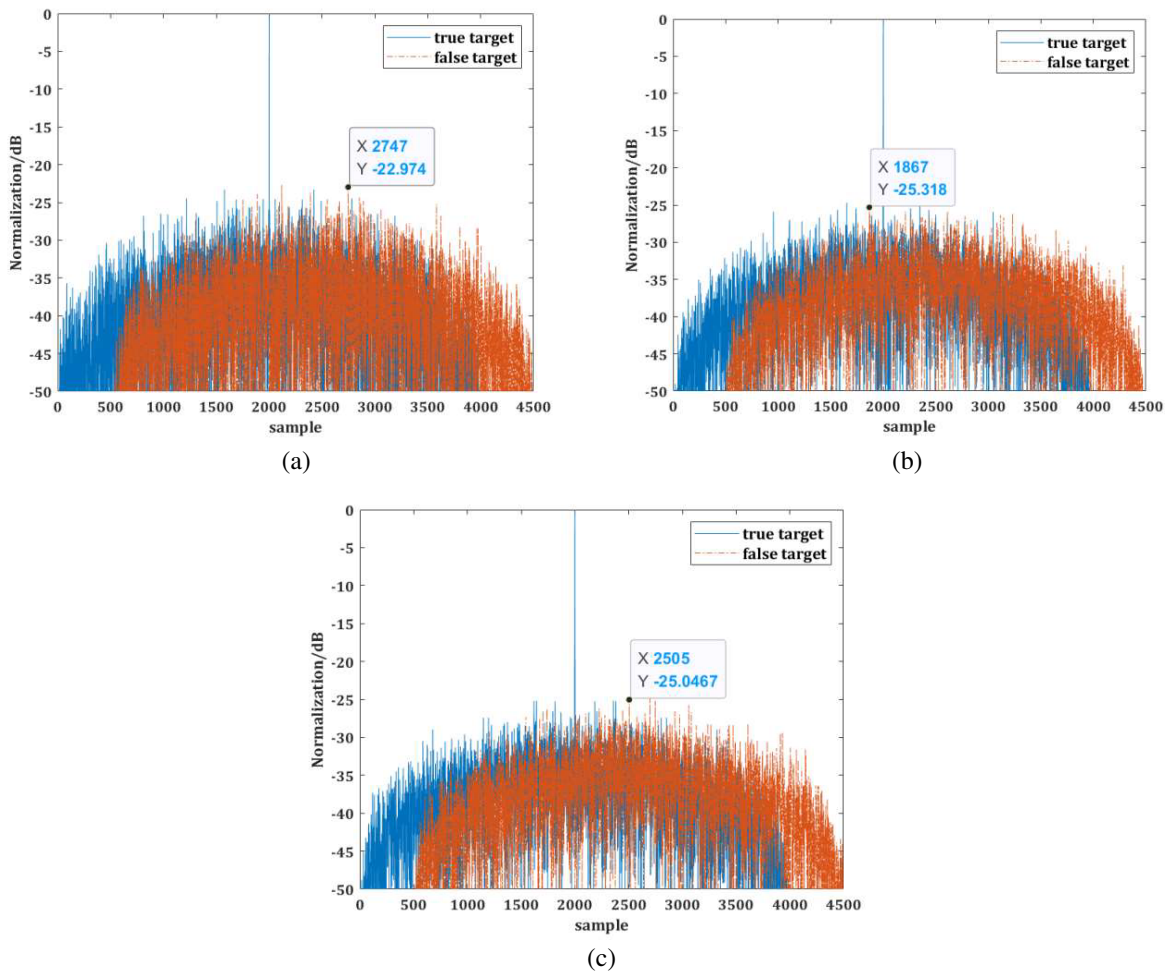


Figure 5. SNR = -6 dB simulation comparison of jamming suppression. (a) LFM, (b) MCPC and (c) MCPC-CS.

From Figure 5, we can see that the duplicated repeater jamming produces a single false target lagging the true target. The three signals can reduce the normalized decibel values of false targets to -22.97 dB, -25.3 dB and -25.04 dB, respectively.

According to Figure 6, δ_{SJR} of MCPC signal is higher than that of LFM signal under different SNR environments. In particular, when the SNR is less than -9 dB, the SJR improvement factor of MCPC and MCPC-CS signals is the same, and they are about 2 dB higher than LFM signals. When the SNR is greater than -9 dB, the SJR improvement factor of MCPC-CS is 0.5 dB ~ 1 dB lower than MCPC, and 5 dB ~ 18 dB higher than LFM signal. At the same time, it can also be concluded from Table 1 that the performance of SJR improvement factor of MCPC signal is more stable than that of LFM signal under different SNR environments.

Table 1. SJR improvement factor in dB.

Signals \ SNRs	SNRs		
	-6 dB	0 dB	6 dB
LFM	19.09	9.46	3.48
MCPC	24.68	23.77	22.18
MCPC-CS	24.56	23.36	21.22

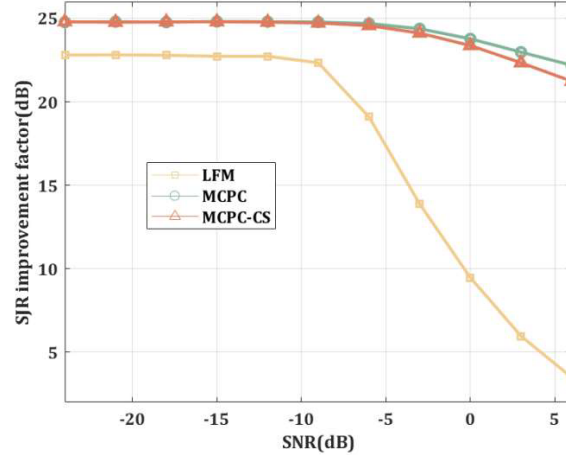


Figure 6. Interference suppression comparison under different SNRs.

4.2. Analysis of Autocorrelation Performance

The autocorrelation performance is evaluated by the ratio of the main side lobe level to the PSLR value of the autocorrelation function. The smaller the PSLR value, the better the autocorrelation performance of the signal.

$$PSLR = \frac{\max_{k \in \text{side-lobe}} |A(k)|}{\max_{k \in \text{main-lobe}} |A(k)|} \quad (13)$$

The simplest way to suppress the autocorrelation sidelobe level of radar waveform is through windowing. Figure 7(a) is the autocorrelation function comparison diagram of LFM signal without window and with Hamming window (H-LFM), and Figure 7(b) is the autocorrelation function comparison diagram of MCPC signal without window and with Hamming window and Schroeder initial phase joint weighting (HS-MCPC).

Although MCPC signal has stronger anti-interference ability than LFM signal, it cannot reduce the autocorrelation sidelobe by 50 dB through simple windowing like LFM signal (Figure 7(a)). This will limit the practical use of MCPC waveform. Therefore, from the perspective of waveform design,

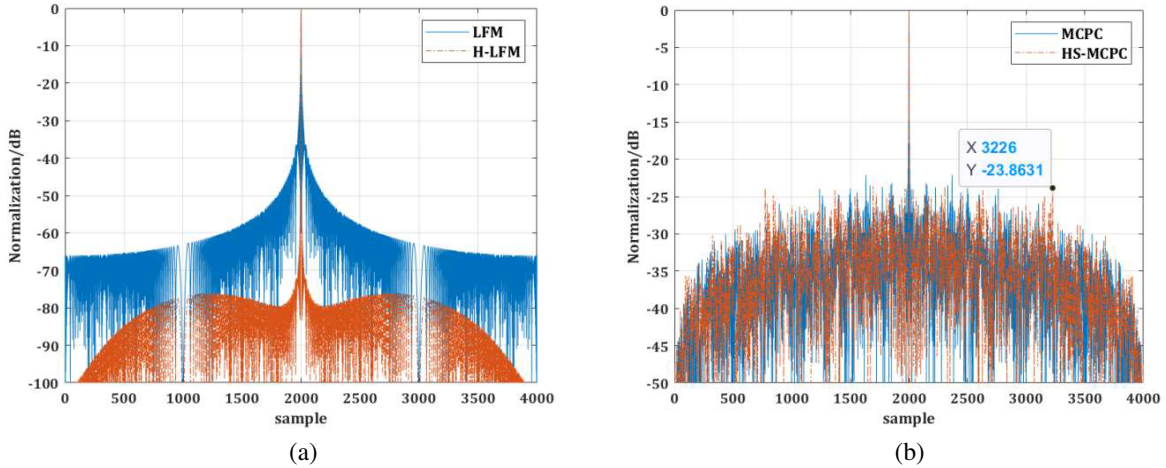


Figure 7. Comparison of autocorrelation performance between windowed and unwindowed conditions. (a) LFM signal, (b) MCPC signal.

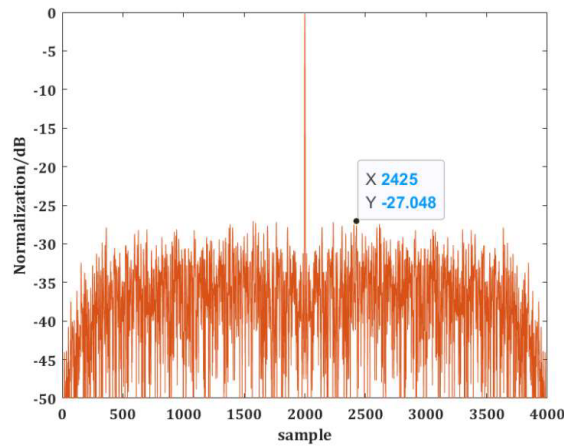


Figure 8. MCPC-CS autocorrelation diagram.

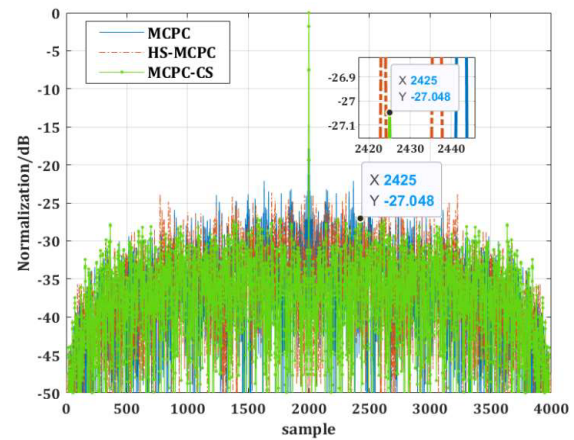


Figure 9. Comparison of three sets of signal autocorrelation performance.

this paper designs MCPC-CS signal to further suppress the autocorrelation sidelobe of MCPC signal based on HS-MCPC waveform. The autocorrelation function of MCPC-CS signal is shown in Figure 8.

From Figure 8 and Figure 9, it can be seen that the PSLR value of MCPC-CS signal is -27.048 dB. Compared with normal MCPC signal and jointly weighted MCPC signal, the PSLR value is reduced by 12 dB and 3 dB, respectively.

Another measure used to evaluate autocorrelation performance is the Integrated Side-lobe level Ratio (ISLR), which is defined as the ratio of total power to peak power of autocorrelation pulse compression side-lobe. For better case, its value should be low and these are calculated as:

$$ISLR = \frac{\sum_{k \in \text{side-lobe}} |A(k)|^2}{|\max A(k)|^2} \quad (14)$$

The autocorrelation performance of MCPC signal and MCPC-CS signal under combined weighting with different parameters is also compared and analysed. The three groups of parameters are 500 MHz/2 μ s, 300 MHz/5 μ s, 64 MHz/128 μ s, respectively. The autocorrelation performance comparison is shown in Table 2.

Table 2. Autocorrelation performance in dB.

Parameters Signals	500 MHz/2 μ s		300 MHz/5 μ s		64 MHz/128 μ s	
	PSLR	ISLR	PSLR	ISLR	PSLR	ISLR
LFM	-13.46	6.93	-13.46	6.93	-13.46	6.93
H-LFM	-50.15	12.90	-50.16	12.90	-50.17	12.90
MCPC	-14.68	12.97	-14.15	13.19	-13.60	13.79
HS-MCPC	-23.63	15.30	-24.29	16.70	-30.28	16.59
MCPC-CS	-27.04	13.62	-27.22	13.19	-33.08	12.96

As can be seen from Table 2, under different parameters, the PSLR value of MCPC-CS signal is always improved by about 3 dB compared with that of MCPC signal. In addition, its ISLR value is smaller than the traditional MCPC signal. Therefore, the MCPC-CS signal designed in this paper is robust.

We compared the method proposed in this paper with other methods, and the results of PSLR are shown in Table 3. Set three groups of different subcarriers, respectively 5×5 , 7×7 , 9×9 .

Table 3. Autocorrelation PSLR in dB.

Parameters Methods	5×5	7×7	9×9
MCPC-CS	-29.93	-29.92	-31.35
HS-MCPC	-26.12	-26.07	-27.51
MCPC-P4 in reference [27]	-13.80	-12.80	-12.80
MCPC-ZC in reference [27]	-15.08	-	-
MCPC-DGP in reference [2]	-26.88	-19.66	-22.38

In [27], Zad-Off Chu polyphase sequence method was proposed to inhibit MCPC autocorrelation sidelobe (MCPC-ZC). This method is improved on the basis of P4 code (MCPC-P4), and it is only suitable for 5 subcarriers [27]. Differential Geometric Progression (MCPC-DGP) proposed in [2] can adapt to multiple subcarriers. When the carrier number of MCPC-CS signal is 5, the autocorrelation PSLR value is -29.93 dB. It is about 14 dB and 3 dB lower than MCPC-ZC method and MCPC-DGP method, respectively. When the carrier number of MCPC-CS signal is 7, the autocorrelation PSLR value is -29.92 dB, which is about 10 dB lower than MCPC-DGP. When the carrier number of MCPC-CS signal is 9, the autocorrelation PSLR value is -31.35 dB. It is about 9 dB lower than MCPC-DGP.

Therefore, the autocorrelation performance of the method designed in this paper is superior to other methods under the number of subcarriers.

5. CONCLUSION

This paper presents an MCPC-CS signal, which is mixed phase modulation by chaotic coding and single coding. MCPC-CS signals have the following advantages: First, the introduction of a single coding can suppress the autocorrelation sidelobes of MCPC signals. After autocorrelation of MCPC-CS signals, the peak sidelobe ratio is 12 dB lower than that of unprocessed MCPC-CS signals, and the distance resolution is improved. Second, due to the pseudo-randomness of chaotic coding itself, the correlation between radar echo and replication-forwarding interference is reduced. Compared with LFM signals, the peak ratio of true target to false target can be improved by about 2 dB. Thirdly, the ambiguity function of MCPC-CS signal presents a “pin” type in peak concentration, which improves the target resolution and accuracy. Finally, MCPC-CS signals are based on MCPC signals, so all the research on MCPC signals can be applied flexibly to the MCPC-CS waveforms proposed in this paper. Based on the above points, the waveform has research value and practicability.

ACKNOWLEDGMENT

This work was supported in part by the Changsha Natural Science Foundation (kq2014111) and Seed Fund of Research and Development Center for Multi-Sensor Intelligent Detection and Recognition Technology (ZZJ202103-02).

REFERENCES

1. Richards, M. A., *Fundamentals of Radar Signal Processing*, McGraw-Hill, New York, NY, USA, 2005.
2. Raghavendra, C. G., R. Prakash, and V. N. Panemangalore, “Reduction of sidelobe levels in multicarrier radar signals via the fusion of hill patterns and geometric progression,” *ETRI Journal*, Vol. 43, No. 4, 650–659, 2021.
3. Argenti, F. and L. Facheris, “Radar pulse compression methods based on nonlinear and quadratic optimization,” *IEEE Transactions on Geoscience and Remote Sensing*, Vol. 59, No. 5, 3904–3916, 2021.

4. Kretschmer, F. F. and B. L. Lewis, "Doppler properties of polyphase coded pulse compression waveforms," *IEEE Transactions on Aerospace and Electronic Systems*, Vol. 19, No. 4, 521–531, 1983.
5. Neuberger, N. and R. Vehmas, "Range sidelobe level reduction with a train of diverse LFM pulses," *IEEE Transactions on Aerospace and Electronic Systems*, Vol. 58, No. 2, 1480–1486, 2022.
6. Di Z., X. Dong, and W. Lin, "Pulse compression with very low sidelobes in a spaceborne weather radar," *International Geoscience and Remote Sensing Symposium (IGARSS)*, Vol. 5, No. 1, V252–V255, 2008.
7. Wang, H., Z. Shi, and J. He, "Compression with considerable sidelobe suppression effect in weather radar," *Eurasip Journal on Wireless Communications and Networking*, No. 97, 2013.
8. Sen S. and C. W. Glover, "Optimal multicarrier phase-coded waveform design for detection of extended targets," *IEEE Radar Conference*, 1–6, 2013.
9. Levanon, N., "Multifrequency complementary phase-coded radar signal," *IEE Proceedings — Radar, Sonar and Navigation*, Vol. 147, No. 6, 276–284, 2000.
10. Huang, Q., Y. Li, W. Cheng, W. Liu, and B. Li, "A new multicarrier chaotic phase coded stepped-frequency pulse train radar signal and its characteristic analysis," *2015 IEEE 10th Conference on Industrial Electronics and Applications (ICIEA)*, 444–448, 2015.
11. Li, D., X. Dai, and H. Zhang, "Sidelobe suppression in NC-OFDM systems using constellation adjustment," *IEEE Communications Letters*, Vol. 13, No. 5, 327–329, 2009.
12. Yang, Z. and J. Tao, "Active point modification for sidelobe suppression with PAPR constraint in OFDM systems," *Wireless Networks*, Vol. 19, No. 7, 1653–1663, 2013.
13. Khan, H. and S. Yoo, "Active interference restriction in OFDM based cognitive radio using genetic algorithm," *2015 International Conference on Information and Communication Technology Convergence (ICTC)*, 840–842, 2015.
14. Tom, A., A. Sahin, and H. Arslan, "Suppressing alignment: Joint PAPR and out-of-band power leakage reduction for OFDM-based systems," *IEEE Transactions on Communications*, Vol. 64, No. 3, 1100–1109, 2015.
15. Prasantha, H. S., "Joint reduction of PMEPR and sidelobe in multicarrier radar signals using ZC and SC method," *WSEAS Transactions on Communications*, Vol. 19, 9–17, 2020.
16. Sivadas, N. A. and S. S. Mohammed, "A joint technique for sidelobe suppression and peak to average power ratio reduction in noncontiguous OFDM based cognitive radio networks," *International Journal of Electronics*, Vol. 104, No. 2, 190–203, 2016.
17. Ni, C., T. Jiang, and W. Peng, "Joint PAPR reduction and sidelobe suppression using signal cancelation in NC-OFDM-based cognitive radio systems," *IEEE Transactions on Vehicular Technology*, Vol. 64, No. 3, 964–972, 2015.
18. Carroll, L. T., "Adaptive chaotic maps for identification of complex targets," *IET Radar Sonar and Navigation*, Vol. 2, No. 4, 256–262, 2008.
19. Huang, Y. L. and Zeng, "Design and characteristic analysis of multicarrier chaotic phase coded radar pulse train signal," *International Journal of Antennas and Propagation*, No. 3, 1–8, 2014.
20. Sun, K., S. He, L. Yin, and L. Duo, "Application of the fuzzyen algorithm to the complexity analysis of chaotic sequences," *Acta Physica Sinica*, Vol. 61, No. 13, 147–203, Chinese Edition, 1984.
21. Li, J., X. Luo, X. Duan, W. Wang, and J. Ou, "A novel radar waveform design for anti-interrupted sampling repeater jamming via time-frequency random coded method," *Progress In Electromagnetics Research M*, Vol. 98, 89–99, 2020.
22. Li, Z. and W. Zou, "An OFDM radar communication integrated waveform based on chaos," *Communications, Signal Processing, and Systems*, 555–562, 2021.
23. Guruswamy, A. and R. Blum, "Ambiguity optimization for frequency-hopping waveforms in MIMO radars with arbitrary antenna separations," *IEEE Signal Processing Letters*, Vol. 23, No. 9, 1231–1235, 2016.

24. Ipanov, R. N., "Polyphase radar signals with ZACZ based on p-Pairs D-Code sequences and their compression algorithm," *Infocommunications Journal*, Vol. 11, No. 3, 21–27, 2019.
25. Yu, M., S. Dong, X. Duan, and S. Liu, "A novel interference suppression method for interrupted sampling repeater jamming based on singular spectrum entropy function," *Sensors*, Vol. 19, No. 1, 136, 2019.
26. Wu, W., J. Zou, C. Jian, S. Xu, and Z. Chen, "False-target recognition against interrupted-sampling repeater jamming based on integration decomposition," *IEEE Transactions on Aerospace and Electronic Systems*, Vol. 57, No. 5, 2979–2991, 2021.
27. Raghavendra, C. G., N. Harsha, and N. N. S. S. R. K. Prasad, "Sidelobe reduction of multicarrier radar signals using Zad-Off Chu polyphase sequence," *International Conference on Inventive Research in Computing Applications*, 1057–1061, 2018.